Available online www.jocpr.com

Journal of Chemical and Pharmaceutical Research, 2015, 7(3):2470-2479

Research Article

ISSN : 0975-7384
CODEN(USA) : JCPRC5

Structural and microstructural properties of Neem husk and seed carbon activated with zinc chloride and phosphoric acid

Alau Kenneth K.*, Gimba Casimir E., Agbaji B. E. and Abeche Steven E.

Department of Chemistry, Ahmadu Bello University, Zaria, Nigeria

---

ABSTRACT

The seed and husk of Neem (Azadirachta indica) are biowastes which have been modified by carbonization and activating it with $ZnCl_2$ and H_3PO_4, to enhance their surface and structural properties, for subsequent application as adsorbent for environmental remediation. Fourier transform Infrared, Scanning electron microscopy, Brauner Emmett Teller and Thermal gravimetric analysis have been carried out to investigate changes and differences in the structure and microstructure of these adsorbents. These techniques indicates that the materials are good and excellent for adsorption purposes.

Keywords: *Activated carbon, Azadirachta Indica, Neem, SEM, BET, FTIR, TGA*

INTRODUCTION

Activated carbon is broadly defined to include a wide range of amorphous carbon based materials prepared in such a way that they exhibit a high degree of porosity and an extended surface area (Bansal, R.P. and Goyal, M. (2005)). The use of activated carbon in its current form has only a short history. On the other hand, according to records, the use of carbon itself dates back to ancient times. The earliest known use of carbon in the form of wood chars (charcoal) by the Egyptians and Sumerians was in 3750 BC (Inglezakis, V.J. and Poulopoulos, S.G. (2006).

Today, activated carbon is very often utilized in the removal of various organic and inorganic species from surface water, groundwater, and wastewater. Most pollutants are difficult to be degradable by natural phenomena of biochemical decomposition. However, pollutants can be attenuated by adsorption on a suitable medium and recovered or isolated through various treatments. Some of the conventional techniques employed include; coagulation and flocculation (Panswed *et al*., 1986), reverse osmosis (Cohen, 1978), chemical oxidation, membrane separation process, electrochemical, and aerobic and anaerobic microbial degradation (Hajira and Muhammed, 2008). All of these methods suffer from one or more limitations (efficiency, cost-effectiveness, availability, management etc.) except 'adsorption' Hajira and Muhammed, (2008). Agricultural by-products such as coconut shell, rice husk, corn cob, groundnut shell, etc have been discovered to be good sources of activated carbon which makes them useful to a host of applications (Hajira and Muhammed, 2008). In a largely agrarian country such as Nigeria, there are so many agricultural by-products lying waste, littering and polluting the environment. The need to further research on these wastes to convert them into agents of environmental control in order to reduce waste and conserve cost is the key to the present research work.

EXPERIMENTAL SECTION

Materials

Samples (Neem husks and seeds) were collected from the National Research Institute for Chemical Technology (NARICT) Zaria while the waste water sample was gotten from University of Abuja Teaching Hospital after certification and approved by the Hospital Ethical Committee. The samples properly washed properly under running tap to remove water-soluble impurities and then dried in a thermostatic oven at 105℃ for 24 hours. The dried samples were pound using mortar and pestle and sieved using a 400 µm mesh sieve.

Chemical Activation of the Neem Carbon

The raw materials (Neem husk and seed) were carbonized at 350^{o}C using a muffle furnace (Carbolite Sheffield England LMF4) which allows limited supply of air. Carbonisation was done at 350^{o}C and for 6 hours. The carbonized samples were allowed to cool at room temperature in a dessicator for three hours before activation.

Chemical activation of the carbonized samples was done at higher temperature using $ZnCl_2$ and H_3PO_4 as activating agents. The carbonized samples were impregnated with the activating agents at room temperature. A carefully weighed amount of the carbonized samples were placed in separate beakers containing each activating agents. The contents of each separate beaker was thoroughly mixed and slightly heated until forms a paste. The paste was then transferred into crucibles which was placed in the furnace and heated at 400^{o}C for 2 hours and then temperature elevated to 600^{o}C for 4 hours. This activated carbon samples was then allowed to cool in a dessicator prior to washing severally with hot distilled water. The washed samples were oven dried at 105^{o}C for 6 hours to constant weight. This was then sieved with a sieves made of brass frame and steel mesh with an aperture of 400μm. The fine sieved samples were stored in a clean airtight container and stored for characterization.

Characterization of Raw Samples

The following physico-chemical tests were used to characterize the sieved samples using standard methods.

Moisture and dry matter content:

Thermal drying at 100℃ and 110℃ in an air circulation oven to constant weight, which is the most common technique (Allen et al., 1974), was employed.

Ash Content:

The ash is the inorganic residue left after the organic matter has been burnt off. The ash content was determined by the method of Allen et al., 1974.

Density and Bulk density:

Bulk density is a measure of density including void pores and interstices and may vary depending on compaction. The bulk density of the sorbents was carried out using the laboratory the method described in the European Committee for Standardization, *CEN/TS 15103*, (2005).

Structural Characterization of Activated Carbon Samples

The following tests were carried out on the structure and morphology of the activated carbon.

Brunauer Emmet Teller (BET) Surface Area: The Brunauer–Emett–Teller (BET) surface area of the activated carbon samples were measured by N_2 adsorption isotherm at 77K using a Micromeritrics Tristar II. The samples were degassed under flowing nitrogen at 250°C for 4hr using a Smart Prep™ 065. The degassing unit removes adsorbed contaminants from the surface and pores of a sample in preparation for analysis. The surface area of the sample was then calculated from the isotherm using the Brunauer–Emett–Teller (BET) equation and N_2 cross-sectional area of 0.162 nm^2.

$$\frac{P_e}{(P_o - P_e)V_{ads}} = \frac{1}{CV_m} + \frac{(C-1)}{CV_m} * \frac{P_e}{P_o}$$

Were P_e is the equilibrium pressure (i.e after sample is exposed to N_2 in manifold), P_o the saturation pressure, V_{ads} the volume of nitrogen adsorbed, V_m the volume of nitrogen monolayer and C is constant.

Fourier Transform Spectroscopy: To study the effect of carbonization and also to investigate the position and presence of characteristic organic groups in the samples' structure, FTIR Analysis was carried out using KBr. The FTIR spectra were recorded on a Shimatzu Fourier Transform Infrared Spectrometer (FTIR) at the National Research Institute for Chemical Technology (NARICT), Zaria. 20 scans were collected for each measurement over the spectral range of 4000-400 cm^{-1} with a resolution of 4 cm^{-1}. All spectra were presented without baseline correction or normalization.

Scanning Electron Microscopy (SEM) for structural morphology of the activated carbon:
The structure and External morphology of the activated carbon samples were determined using Quanta Scanning Electron Microscope FEI Quanta 250 and carried out at the School of chemistry and Chemical engineering Queens University, Belfast.

Thermogravimetric Analysis (TGA): Thermal characterizations of the adsorbent samples were performed using Mettler-Toledo TGA/DSC I STAR^e instrument with heating rate of 20ºC/min in nitrogen (N_2) atmosphere. Thermal Analysis (TGA and DSC) detects the inter-atomic and inter-/intra- molecular interactions as related to an imposed external change in temperature.

RESULTS AND DISCUSSION

Table 1: Physicochemical parameters of the Neem (*Azadirachta indica*) husk and seed:

	RNH	RNS	NHZ	NSH	NHZ	NHH
Moisture content (%)	4.45	8.95	3.62	3.67	3.05	3.02
Dry matter (%)	95.55	91.05	96.38	96.23	96.95	96.98
Volatile Matter Content (%)	54.44	53.10	9.81	10.14	12.06	3.89
Ash Content (%)	11.33	6.56	18.70	18.60	18.34	20.11
Fixed Carbon Content (%)	29.78	25.62	67.87	67.49	66.55	72.98
Particle size (µm)	400	400	350	350	350	350
Bulk density (g/cm^3)	0.95	0.87	0.77	0.83	0.76	0.82

N_2 Adsorption Isotherms of Activated Carbon
The N_2 adsorption isotherms of the activated carbon samples are summarized in Table 2. Identifying pore structure of adsorbents by the adsorption of inert gases is essential before sorption experiments. Table 2 presents the BET surface area, pore volume, and pore size of NSH, NSZ, NHZ and NHH obtained from N_2 adsorption isotherms. The BET surface area for NHH, NHZ, NSH and NSZ were found to be 233.22, 241.44, 252.18 and 353.98m^2/g respectively while the average pore sizes were also found to follow similar pattern of 22.22, 24.16, 22.46 and 34.14Å for NHH, NHZ, NSH and NSZ respectively. The results indicate that the activated carbon from the Neem materials are reasonably good for adsorption. The samples show a high proportion of micropore volume (about 90% of total pore volume) and means that activated carbon indicates a higher volume of wide micropores and presence of small mesopores. The pore diameter of the activated carbon was found to be between 22Å and 34Å, indicating that the activated carbon prepared was in the mesopores region according to the International Union of Pure and Applied Chemistry (IUPAC), pores are classified as micropores (<20 Å), mesopores (20–500 Å) and macropores (>500 Å) (Ahmad and Hameed, 2009). Mesopore development induced by phosphoric acid and zinc chloride has also been reported by other studies (Teng et al., 1998; Timur et al. 2006).

Table 2: BET result of Neem activated carbon

Figure 4.1:	Agent	R^2	Type	Qm	BET_{SA} (m2/g)	P_{vol} cm3/g)	P_{Size} (Å)
Neem Husk	H_3PO_4	0.9969	II	53.02	230.79	0.010752	22.221
	$ZnCl_2$	0.9966	II	54.80	238.56	0.009838	22.456
Neem Cake	H_3PO_4	0.9967	IV	80.87	352.00	0.0472	34.26
	$ZnCl_2$	0.9966	II	57.93	252.18	0.014657	24.155

Agent represent the Activating agent; R^2 is the coefficient of regression; *Type* represents the adsorption Isotherm type; BET_{SA} represents the Brunauar-Emmet-Teller surface area of the adsorbents; Q_m is the monolayer Quantity of gas adsorbed; P_{vol} is the pore volume of the adsorbent and P_{size} is the calculated Pore sizes of the materials.

Fourier Transform Infrared (FTIR) Analysis
Fourier transform infrared spectroscopy (FTIR) was used to determine the vibration frequency changes in the functional groups in the carbons. The spectra of carbons were measured within the range of 400–4000 cm^{-1}. Spectra plots for the adsorbents are shown in Figure 1 to 6. Table 3 lists the fundamental frequencies of the raw Neem samples and AC samples indicating their band frequencies in the FTIR spectrum. The FTIR spectrum obtained for the prepared activated carbon displayed major absorption bands at 3400-3800 cm^{-1}, 2200-2400 cm^{-1}, 1500-1700 cm^{-1}, 1000-1200 cm^{-1} and 450-750 cm^{-1}. A wide band with two maximum peaks can be noticed at about 3450 and 3855 cm^{-1}.

The bands at 400-483 cm^{-1} and 500-800 cm^{-1}are associated with the inplane and out-of-plane aromatic ring deformation C-H bending mode. The broad bands between 700 and 800 cm−1 represents bounded O–H groups in the carbon structure. In the raw samples the strong peak seen at 1420-1460 cm−1has been assigned to stretching vibrations of C-C bonds. The disappearance of these bands is evident of successful carbonization. On the other hand, C–H stretch could be ascribed to the band that appeared at 1000-1100 cm−1. The band at 1500 cm^{-1} may be attributed to the aromatic rings carbon–carbon stretching vibration enhanced by polar functional groups (Prahas et al., 2008; Ahmad and Hameed, 2009). The strong peaks around 1600 cm^{-1} has not been clearly interpreted. It refers to stretching vibrations of bonds in the aromatic ring coupled to that of highly conjugated carbonyl groups (C=O) (Sahira et al., 2013). The strong band around 1720 cm^{-1} found in the raw samples shows the presence of stretching vibration of C=O bonds in ketones, aldehyde, lactone, and carboxyl (Prahas et al., 2008, Sahira et al., 2013) . These groups are abundant in the raw samples. Disappearance of these peaks in the activated carbon samples is indicative of complete carbonization.

The peaks at 2250-2400 cm −1 denotes C O stretching from ketones, aldehydes or carboxylic groups in the raw samples and the interaction between Oxygen and carbon during pyrolysis in the activated carbon samples. Oxygen containing surface functional groups plays important role in influencing the surface properties and adsorption behaviour of the samples though amples were prepared via the different activation methods. The nature of activating agents do not have much effect in the type of oxygenated surface functional groups (Sahira et al., 2013). The weak peak in the raw samples around 2900 cm^{-1} is attributed to C-H (stretching vibration in methyl group) interaction with the surface of the carbon. The groups disappear after pyrolysis. The band aroun 3450 cm- 1 is due to the absorption of water molecules as result of an O-H stretching mode of hydroxyl groups and adsorbed water. Likewise Weak band around 3740 cm^{-1} is assigned to stretching vibration of O-H bonds in hydroxyl groups (Ahmad and Hameed, 2009; Sahira et al., 2013). The location of hydrogen-bonded OH groups, usually in the range of 3200–3750 cm−1 for alcohols and phenols, involved in hydrogen bonding may be due to adsorbed water.

The FTIR spectra obtained was in agreement with the results reported in the studies carried out on activated carbons prepared from rice straws (Wang et al., 2007; Gao et al., 2011) Oak sawdust (Abd El-Latifa et al., 2010) and coconut tusk (Abechi et al., 2013). From the spectra of activated Carbon samples, it can be noted that all carbons contain oxygenated surface functional groups such as hydroxyl, carbonyl, carboxyl and lactones (Sahira et al., 2013). These acidic surface functional groups are favourable for removal of color and COD (Ahmad and Hameed, 2009). There are significant changes of the absorption band from raw material compared with activated carbon product but the spectra show that the surface functional groups of the activated carbons do not exhibit significant differences, independently of the activating agent used. Only slight differences on the intensity of the bands were detected.

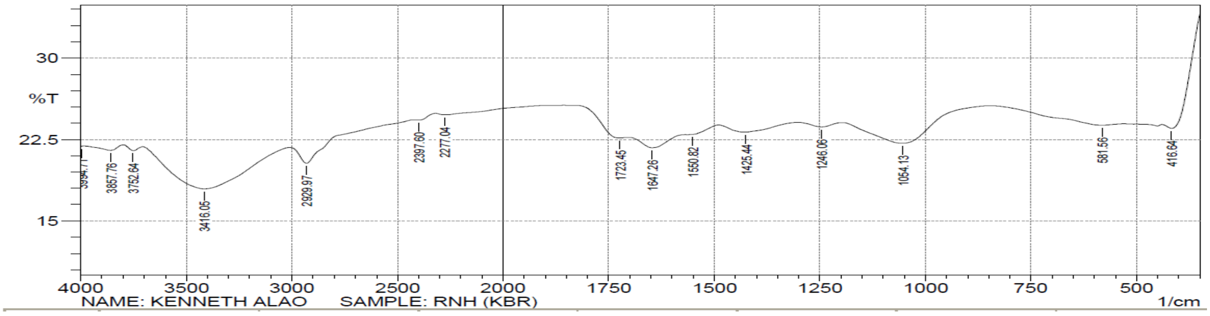

Figure 1: Fourier Transform Infrared Spectroscopy (FTIR) – Raw Neem Husk

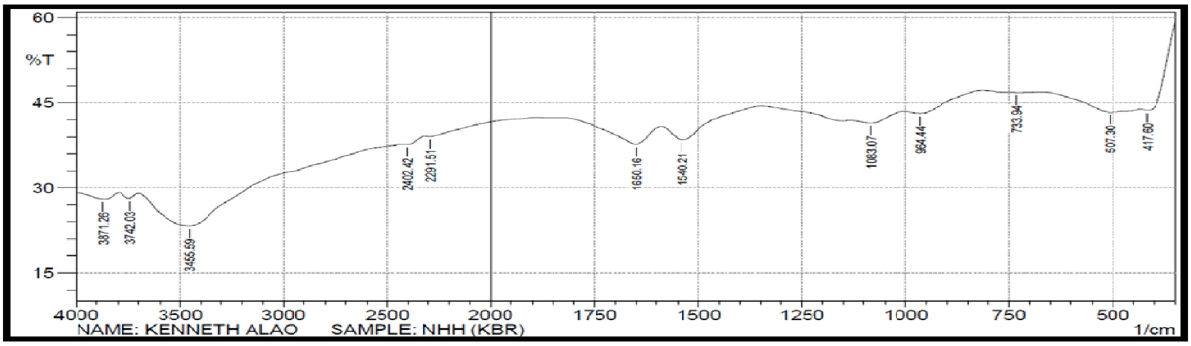

Figure 2: Fourier Transform Infrared Spectroscopy (FTIR) – Neem husk activated with $ZnCl_2$

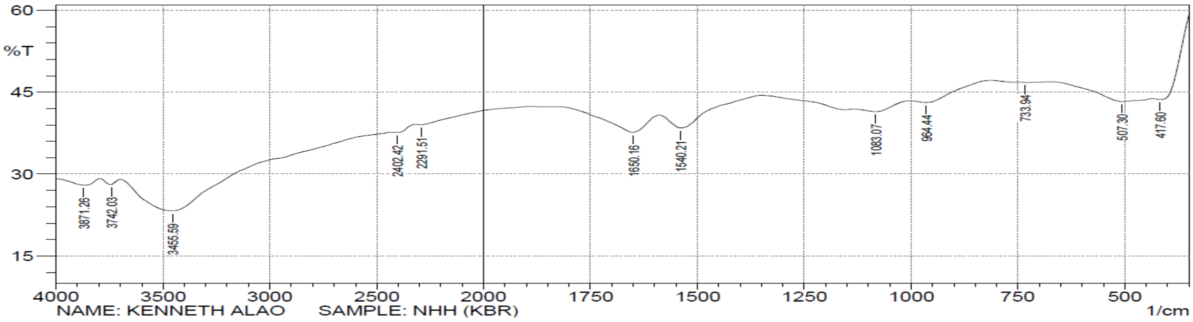

Figure 3: Fourier Transform Infrared Spectroscopy (FTIR) – Neem husk activated with H_3PO_4

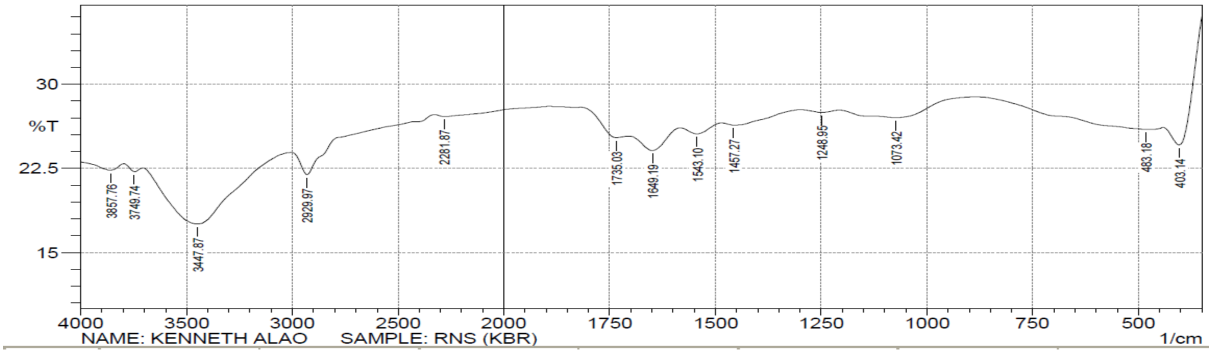

Figure 4: Fourier Transform Infrared Spectroscopy (FTIR) – Raw Neem cake

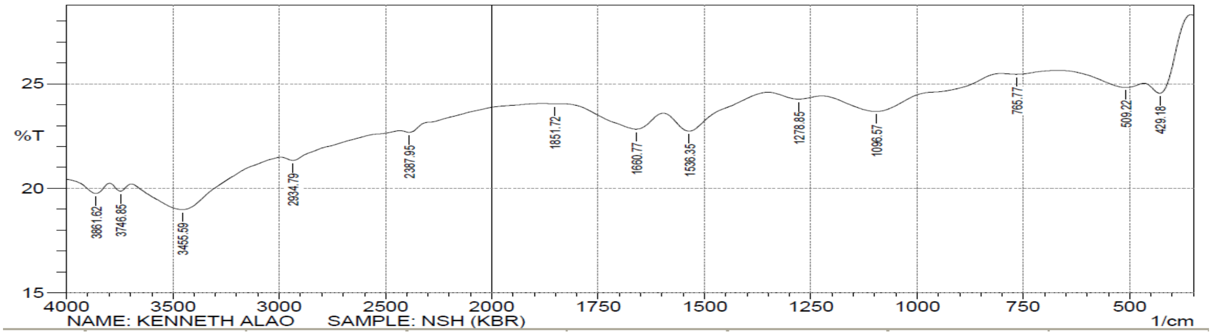

Figure 5: Fourier Transform Infrared Spectroscopy (FTIR) – Neem cake activated with H_3PO_4

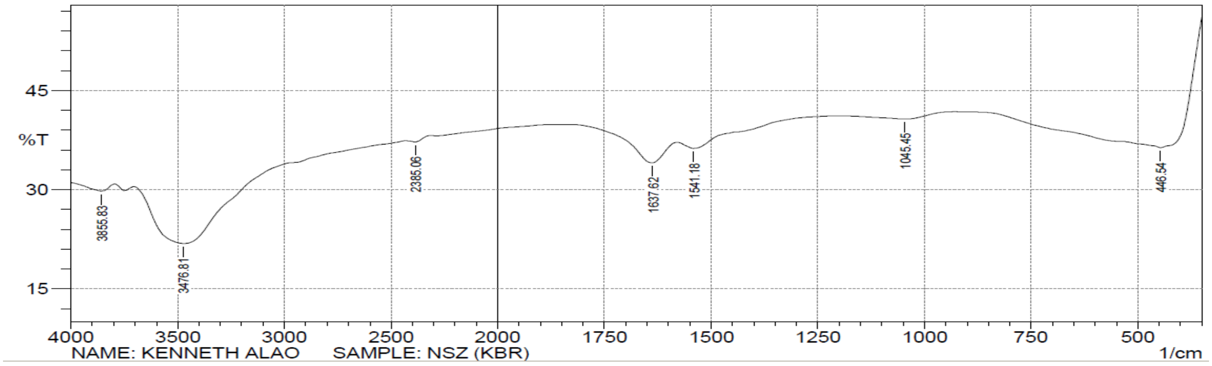

Figure 6: Fourier Transform Infrared Spectroscopy (FTIR) – Neem cake activated with $ZnCl_2$

Table 3: FTIR Table of assignment

Position (cm^{-1})	Vibration	Inference
800-400	C-H bending	inplane and out-of-plane aromatic ring deformation
1100-1000	CH stretching	Lignocellulose
1200*	CH stretching	Cellulose, hemicellolose
1460-1400*	C=C stretching	Unsaturated carboxylic acids and oils
1500	C-C	Polar functional groups
1660-1620	C=O stretching	Carbonyls, weak C=O bonds from pyrolysis
1745*	C=O	Carboxylic acids and carbonyls
2400-2200	C=O stretching	Carbonates, carbonyls, esters
2900	C-C Stretch	Methyl group
3824-3440	O-H stretching	Surface and rapped OH. moisture, phenols, Alcolhols

**vibrations that disappeared completely after activation.*

Scanning Electron Microscopy (SEM)

Figures 7 to 14 show the SEM micrographs of the neem and neem husk derived activated carbon. The SEM enables the direct observation of the changes in the surface microstructures of the carbons due to the modifications (Goel et al., 2005). Many large pores in a honeycomb shape were clearly found on the surface of the activated carbon. The well-developed pores had led to the large surface area and porous structure of the activated carbon (Ahmad and Hameed, 2009). There is clear demarcation in the surface morphology of AC treated with $ZnCl_2$ and H_3PO_4. The morphology of NHZ and NSZ as can be observed from Figures 7 to 14, clearly showed developed honey comb like, highly defined cylindrical pores and cavities and rough surfaces on the carbon samples. The largely isolated cylindrical units have walls made up of layers of relatively thick sheets. This demonstrated that $ZnCl_2$ was effective to create well developed pores with uniform distribution leading to large surface area and porous structure.

The morphology of NHH and NSH were bulky, sponge-like with large surfaces and narrow pores widths. The narrowing of the pore widths suggest a kind of deformation where the matrix softens and walls of the pores give way and close in on each other. For NHH and NSH, the phosphoric acid incorporated into the interior of the precursor particle restricted the formation of tar as well as other liquids such as acetic acid and methanol, present in the raw neem material, and inhibited the particle shrinkage or volume contraction during heat treatment. Another important feature of the NSH micrographs is the cracks in the carbon matrix probably developed as a result of thermal stress on the carbon matrix due to temperature changes in the activation process. Such cracks contribute to the overall surface of the activated carbon and as such are important. The cavities on the surfaces of carbons resulted from the evaporation of the activating agent (phosphoric acid) during carbonization, leaving the space previously occupied by the activating agent (Prahas et al., 2008). On one hand, the restricted shrinkage and limited volatile released might facilitate the conservation of porous structures present in the precursor. On the other hand, after washing the final product, the extraction of deeply penetrated acid led to the creation of tremendous porosity. Activated carbons with an enhanced mesoporosity can also be obtained from phosphoric acid activation.

Figure 7: Micrograph of the transverse section of Neem seed activated with $ZnCl_2$

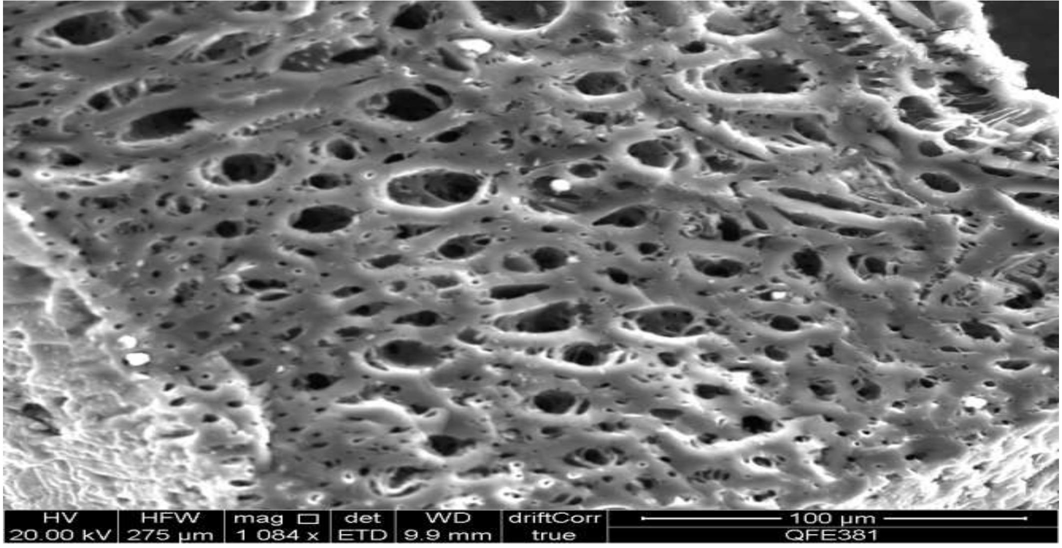

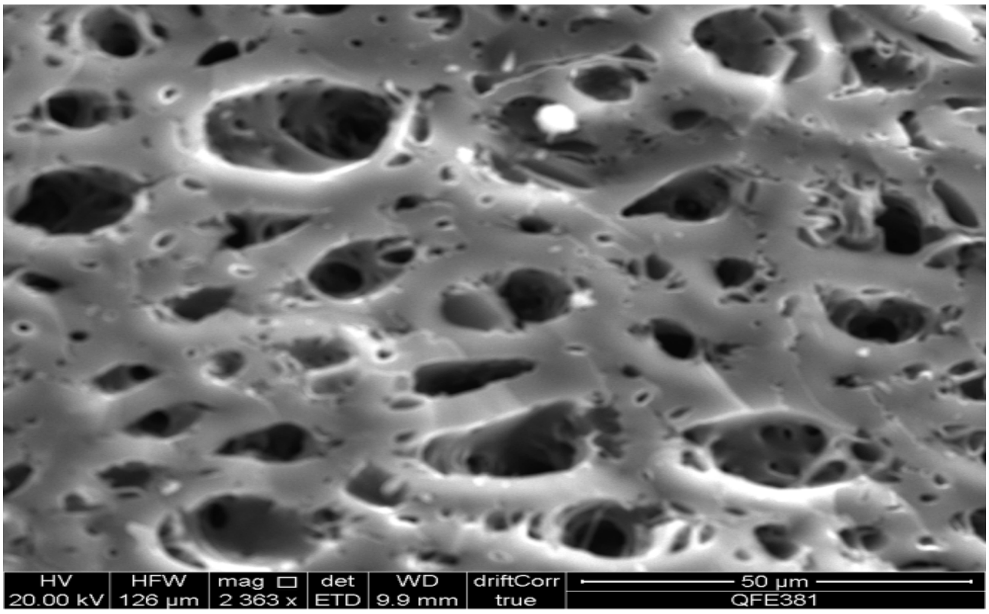

Figure 8: Micrograph of the transverse section of Neem seed activated with $ZnCl_2$

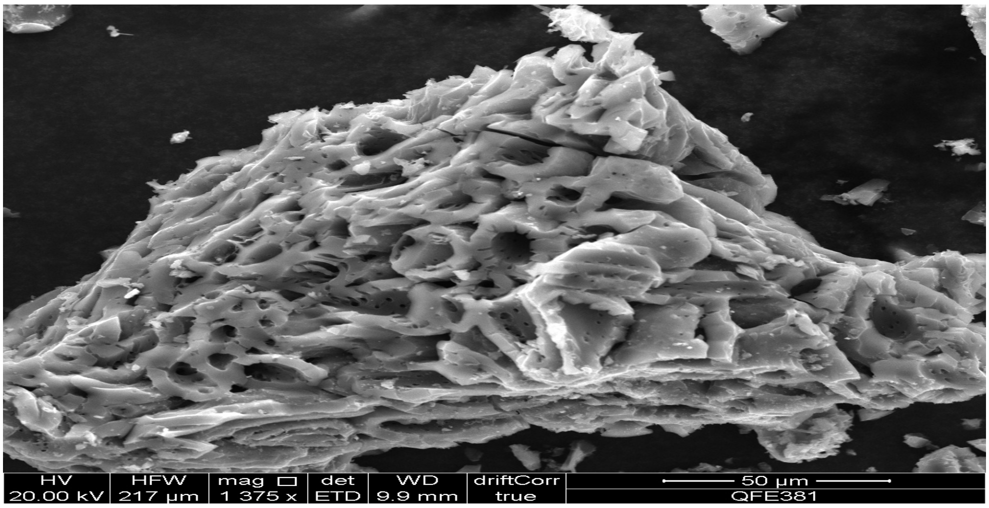

Figure 9: SEM of Neem husk activated with $ZnCl_2$

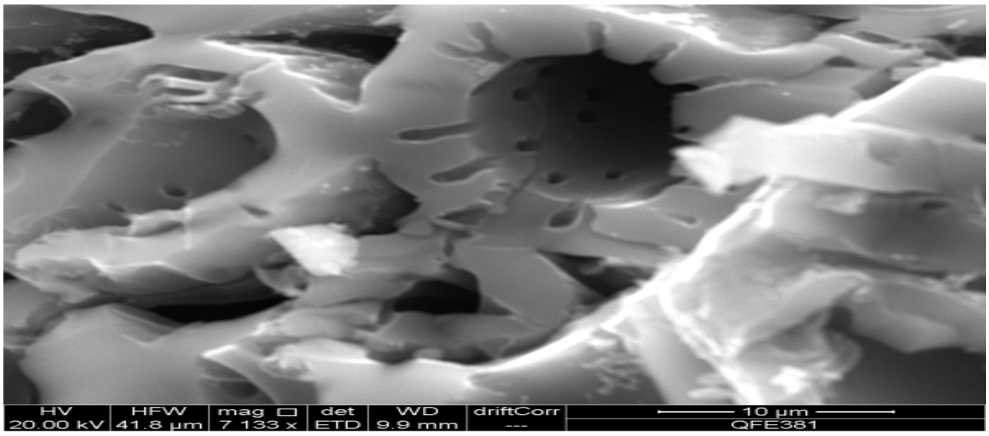

Figure 10: SEM of Neem husk activated with $ZnCl_2$

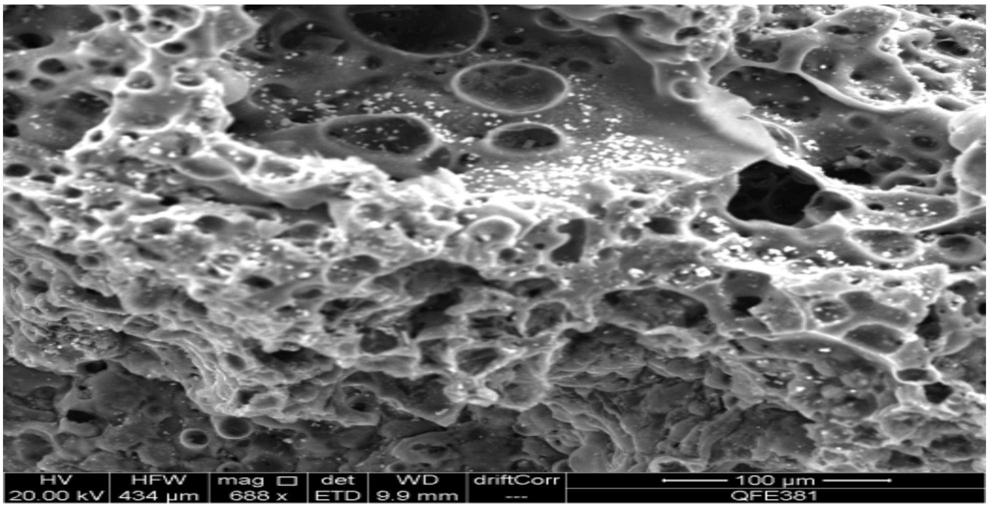

Figure 11: SEM of Neem husk activated with H_3PO_4

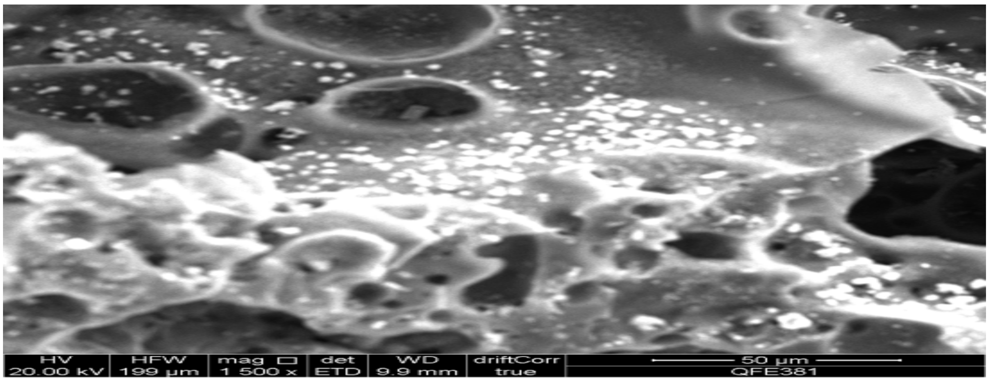

Figure 12: SEM of Neem husk activated with H_3PO_4

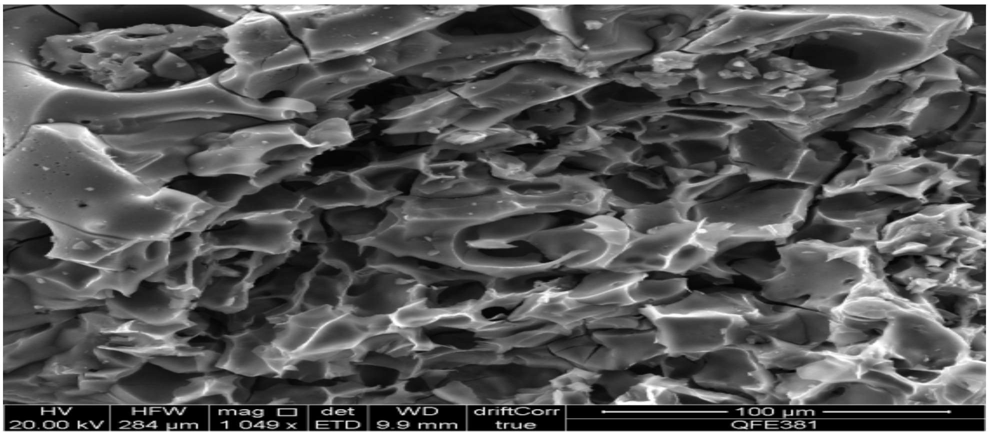

Figure 13: SEM of Neem seed activated with H_3PO_4

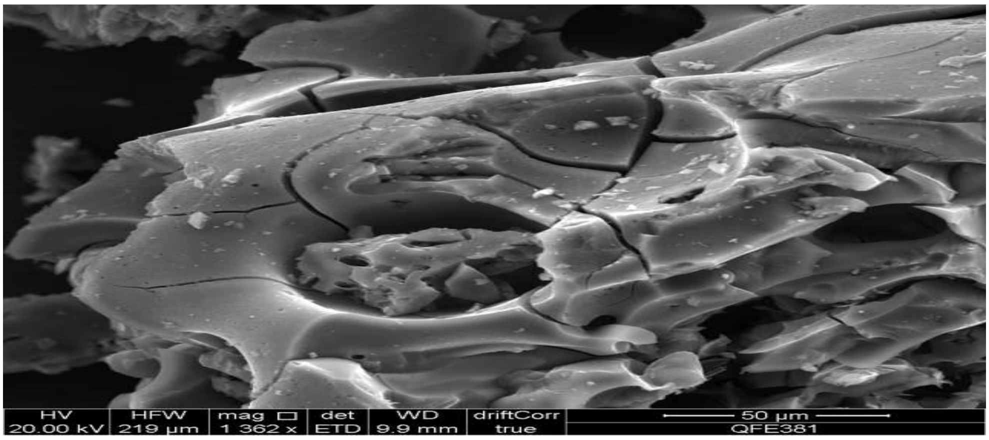

Figure 14: SEM of Neem seed activated with H_3PO_4

Thermo-Analytical Studies

The thermal stability of the activated carbon samples were tested by measuring the mass loss during a heating ramp rate. The descending TGA thermal curves indicate the occurrence of weight loss. The details of the Thermograms are presented in Table 4. Two stages of thermal decomposition behaviour have been studied and revealed two derivative peaks in temperature in the TG curve of each samples. The mid-points for the first derivative peak temperatures were 87.00°C , 85.64°C , 88.35°C and 86.86°C for NSZ, NSH, NHZ and NHH respectively. The values of the Zinc Chloride activated carbon samples tend to be more hydrophobic and slightly more resistant to heat than their corresponding Phosphoric acid activated carbon samples. A 3.62%, 3.67%, 3.05% and 3.02% of weight loss occurred in NSZ, NSH, NHZ and NHH respectively, in the temperature range of 50°C to 350°C. The weight loss at this range is usually due to moisture being dried off in the material. The mid-points for the second derivative peak temperatures were 450.01, 449.55, 465.23 and 466.19°C for the activated carbon samples NSZ, NSH, NHZ and NHH respectively, resulting to an overall mass loss of 9.81, 10.14, 12.06 and 3.89% respectively, which is about 10 times higher than the weight loss that was recorded at the earlier peak. The total weight loss in the NHH sample proved it to be the most thermally stable material. At temperatures ranging from 350°C to 500°C, the huge weight loss could be attributed to the decomposition of organic components in the raw material, such as cellulose, hemicelluloses, and lignin.

Table 4: TGA/DTG points

Sample	Stage 1 (0-350 ºC)			Stage 2 (350-500 ºC)			DTG values	
	Step (%)	Inf. Pt. (ºC)	Mid Pt. (ºC)	Step (%)	Inf. Pt. (ºC)	Mid Pt. (ºC)	Peak (ºC)	Peak Val x10^{-3} (mg/min)
NSZ	3.62	81.47	87.00	9.81	493.68	450.01	81.16	-93.35
NSH	3.67	79.23	85.64	10.14	493.4	449.55	80.78	-80.15
NHZ	3.049	81.01	88.55	12.06	496.46	465.23	79.45	-69.37
NHH	3.02	76.55	86.87	3.89	492.78	466.19	75.94	-41.36

Step represent the % weight loss of the sample in that stage; Inf. Pt. is the inflection point of thermal degradation; Mid Pt. is the Mid Point of the thermal degradarion; DTG stands for diffential thermal gravimetry.

CONCLUSION

The studied parameters (moisture content, dry matter, ash content, bulk density, surface area and TGA) of the raw neem husk and seed were observed to be different relative to the activated sample. This shows that the carbonization and activation process was successful and effective when compared to the commercial adsorbents and other adsorbents form agricultural waste as cited in literatures. It was also observed that the Neem seed activated carbon showed better results than the Neem husk results. These results were confirmed by the SEM results which showed the microstructural morphology of the activated carbon samples showing large honey-like pores and thick surfaces. FTIR result proved the change in the chemical properties of the raw carbon samples. There was reduction in volatile matter content which was made evident by the disappearance of special bands at about 1200, 1400 and 1700 cm^{-1}.

REFERENCES

[1] Abd El-Latifa, M. M., & Ibrahim, A. M. (**2010**). *Desalination and Water Treatment*, 20(1-3), 102-113.

[2] Ahmad, A.A. and Hameed, B.H. (**2009**). *Journal of Hazardous Materials*. 172, 1538–1543.

[3] Alau, K. K., Gimba, C. E., Kagbu, J. A., & Nale, B. Y. (**2010**). *Archives of Applied Science Research*, 2(5), 451-455.

[4] Allen, S. E., Grimshaw, H. M., Parkinson, J. A., & Quarmby, C. L. (**1974**). Chemical analysis of ecological materials. Blackwell Scientific Publications.
[5] Ekpete, O. A., & Horsfall, M. J. N. R. (**2011**). *Res J Chem Sci*, 1(3), 10-17.
[6] El-Hendawy A.A., Samra S.E., Girgis B.S. (**2001**). *Colloid Surface A: Physicochem Eng Aspects*, 180: 209–21.
[7] Gao, P., Liu, Z. H., Xue, G., Han, B., & Zhou, M. H. (**2011**). *Mater Lett*, 57: 164–72.
[8] Goel J., Kadirvelu, K., Rajagopal C., Garg V. K. (**2005**). *Journal of Hazardous Materials* B, 125, 211–220.
[9] Prahas, D., Kartika, Y., Indraswati, N., and Ismadji, S. (**2008**). *Chemical Engineering Journal*, 140(1), 32-42.
[10] Roop Chand Bansal and Meenakshi Goyal (**2005**). Activated Carbon Adsorption. Published in 2005 by CRC Press Taylor and Francis Group 6000 Broken Sound Parkway NW, Suite 300 Boca Raton, FL 33487-2742.
[11] Sahira, J., Mandira, A., Prasad, P. B., & Ram, P. R. (**2013**). *Research Journal of Chemical Science*, 3(5), 19-24
[12] Teng, H., Yeh, T.S., Hsu, L.H., (**1998**). *Carbon*, 36, 1387-1395.
[13] Timur, S., Kantarli, I.C., Ikizoglu, E., Yanik, J., (**2006**). *Energy and Fuels*, 20, 2636-2641.
[14] Tsai WT, Chang CY, Wang SY, Chang CF, Chien SF, Sun HF (**2001**). *Resour Conserv Recy*, 32: 43–53.